PROCESS DESIGN AND CONTROL

Extended Kalman Filter-Based Nonlinear Model Predictive Control for a Continuous MMA Polymerization Reactor

Sung-Mo Ahn, Myung-June Park, and Hyun-Ku Rhee*

School of Chemical Engineering and Institute of Chemical Processes, Seoul National University, Kwanak-ku, Seoul 151-742, Korea

A mathematical model was developed for a continuous reactor in which free radical polymerization of methyl methacrylate (MMA) occurred. Elementary reactions considered in this study were initiation, propagation, termination, and chain transfers to monomer and solvent. The reactor model took into account the density change of the reactor content and the gel effect. To measure the conversion and weight-average molecular weight on line, the on-line densitometer and viscometer were installed in such a way that the measured values of density were used to calculate the conversion and the viscosity measurement along with conversion data was used to determine the weight-average molecular weight. A control system was designed for a continuous reactor using an extended Kalman filter (EKF)-based nonlinear model predictive controller (NLMPC) to control both the conversion and the weight-average molecular weight of the polymer product. The control input variables were the jacket inlet temperature and the feed flow rate. For the purpose of validating the control strategy, an on-line digital control experiment was conducted with an on-line densitometer and viscometer installed. Despite the complex and nonlinear features of the polymerization reaction system, the EKF-based NLMPC performed quite satisfactorily for the property control of the continuous polymerization reactor.

1. Introduction

Continuous polymerization reactors are widely used to produce synthetic polymers. With an increasing demand for high-quality polymers, it is necessary to build a control strategy that would give a good control of the properties of the polymer product and that would minimize the production of off-spec polymer during the start-up or grade change operations. However, polymerization processes are difficult to control effectively due to their severe nonlinearity. As a result, several kinds of nonlinear control strategies have been developed for polymerization processes.

A feedforward and feedback control scheme was designed by Congalidis et al.[1] to regulate polymer production rate, molecular weight, and reactor temperature. They used the solution copolymerization of methyl methacrylate (MMA) and vinyl acetate in a continuous stirred tank reactor as an illustrative example with the kinetic parameters and reactor operating conditions obtained from the literature. Adebekun and Schork[2,3] had demonstrated a nonlinear estimation and control method to be suitable for the control of a continuous MMA polymerization reactor. They obtained satisfactory results even when the desired steady state was open-loop unstable. A cascade model reference adaptive algorithm was proposed by Elicabe and Meira[4] to control a continuous polymerization reactor, which was operated under forced oscillations of its feeds. Their computer simulations demonstrated the feasibility of the proposed technique, provided continuous state measurements were available. Kurtz and Henson[5] controlled monomer concentration and reactor temperature using a technique which combined input–output decoupling and linear model predictive control. They used an input–output decoupling to obtain a linear model between the outputs and a vector of new inputs.

Despite all these simulation studies, there have been only a few published reports on the actual implementation of such control schemes to the continuous polymerization reactor systems through experiments. The globally linearizing control (GLC) method was implemented to control conversion and temperature by Soroush and Kravaris[6] through experimental study. They proposed a correlation to determine conversion from density and temperature measurements and studied the performance of the controller in the presence of active input and state constraints. Mutha et al.[7] designed the control strategy to handle the control of nonaffine systems (nonlinear in the manipulated variables). They presented an experimental evaluation of a nonlinear model-based estimator and a predictive control strategy on a continuous MMA solution polymerization reactor.

From the review of earlier works, it is apparent that what is in demand is not only a more effective control algorithm for the properties of the polymer product but also actual implementation of the control strategy on the continuous polymerization reactor system.

In this study, the extended Kalman filter (EKF)-based nonlinear model predictive controller (NLMPC)[8] was implemented experimentally to control the conversion and the weight-average molecular weight of the polymer product in a continuous methyl methacrylate (MMA)

---

* To whom all correspondence should be addressed. Telephone: +82-2-880-7405. Fax: +82-2-888-7295. E-mail: hkrhee@snu.ac.kr.

polymerization reactor. The manipulated variables were the jacket inlet temperature and the feed flow rate. To measure the properties of the polymer on line, the densitometer and the viscometer were utilized.

2. Polymerization Reactor Model

In this section, we considered a continuous stirred tank reactor for MMA polymerization. The reaction kinetics are assumed to follow the free radical polymerization mechanism including chain-transfer reactions to both solvent and monomer.

From the general free radical polymerization mechanism, the following mass balance equations can be derived for the initiator, the monomer, and the solvent:

$$\frac{d(IV)}{dt} = q_f I_f - qI - k_d IV \tag{1}$$

$$\frac{d(MV)}{dt} = q_f M_f - qM - \{2fk_d I + (k_p + k_{trm})MG_0\}V \tag{2}$$

$$\frac{d(SV)}{dt} = q_f S_f - qS - k_{trs}SG_0 V \tag{3}$$

in which V and q denote the volume of the reaction mixture and the volumetric flow rate, respectively, while I, M, S, and G_0 represent the concentrations of initiator, monomer, solvent, and living polymer, respectively. The subscript f denotes the feed stream.

To describe the molecular weight distribution, it is not necessary to solve the infinite number of equations for the concentration of polymer chains of each length. Instead, the method of moments was adopted to calculate the number-average molecular weight (M_n) and the weight-average molecular weight (M_w). The definitions of the moments are as follows:

$$G_k = \sum_{n=1}^{\infty} n^k R_n(t) \quad \text{and} \quad F_k = \sum_{n=1}^{\infty} n^k P_n(t), \quad k = 0, 1, 2 \tag{4}$$

where G_k and F_k are the kth moments of living and dead polymer concentrations, respectively. One can derive balance equations for the first three moments of the living and dead polymer concentrations as follows:

$$\frac{d(G_0 V)}{dt} = -qG_0 + \{2fk_d I - k_t G_0^2\}V \tag{5}$$

$$\frac{d(G_1 V)}{dt} = -qG_1 + \{2fk_d I + k_p MG_0 - k_t G_0 G_1 + (k_{trm}M + k_{trs}S)(G_0 - G_1)\}V \tag{6}$$

$$\frac{d(G_2 V)}{dt} = -qG_2 + \{2fk_d I + k_p M(G_0 + 2G_1) - k_t G_0 G_2 + (k_{trm}M + k_{trs}S)(G_0 - G_2)\}V \tag{7}$$

$$\frac{d(F_0 V)}{dt} = -qF_0 + \left\{\frac{1}{z}(k_t + k_{td})G_0^2 + (k_{trm}M + k_{trs}S)G_0\right\}V \tag{8}$$

$$\frac{d(F_1 V)}{dt} = -qF_1 + \{(k_t G_0 + k_{trm}M + k_{trs}S)G_1\}V \tag{9}$$

$$\frac{d(F_2 V)}{dt} = -qF_2 + \{(k_{td}G_0 + k_{trm}M + k_{trs}S)G_2 + k_{tc}(G_0 G_2 + G_1^2)\}V \tag{10}$$

As the monomer is converted to polymer, the density of the reactor content increases as the reaction proceeds. The volume change of the reaction mixture may be expressed by the following equation:[9]

$$\frac{dV}{dt} = q_f\left(\frac{M_f w_m}{\rho_m} + \frac{S_f w_s}{\rho_s}\right) - q + \left[r_M w_m\left(\frac{1}{\rho_m} - \frac{1}{\rho_p}\right)\right]V \tag{11}$$

in which w and ρ denote the molecular weight and the density, respectively, whereas the subscripts m, s, and p represent the monomer, the solvent, and the polymer, respectively. The rate of monomer formation r_M is given by the expression inside the brackets on the right-hand side of eq 2. In this study the reactor is operated in such a way that the reaction mixture flows out of the reactor via an overflow line. Hence, eq 11 with $dV/dt = 0$ is used to determine q as a function of the time. For the gel effect, we adopted the correlations proposed by Schmidt and Ray.[10]

The temperature dependence of the rate constants is assumed to follow the Arrhenius law. The kinetic data used for the plant model of this study are taken from the literature.[11] On the basis of the mass balance equations, the conversion and the number- and weight-average molecular weights are defined as follows:

$$X = \frac{V_p \rho_p}{V \rho_r} \tag{12}$$

$$M_w = w_m \times \frac{(G_2 + F_2)}{(G_1 + F_1)} \tag{13}$$

$$M_n = w_m \times \frac{(G_1 + F_1)}{(G_0 + F_0)} \tag{14}$$

where the subscript r denotes the reaction mixture.

The energy balances for reactor and jacket can be formulated as follows:

$$\frac{d(V(\rho C_p)_{mean}T_r)}{dt} = (\rho C_p)_{mean}q_f T_f - (\rho C_p)_{mean}qT_r + V(-\Delta H)k_p MG_0 - UA(T_r - T_j) + Q_{loss} \tag{15}$$

$$\frac{d(V_j(\rho C_p)_c T_j)}{dt} = (\rho C_p)_c q_c T_j^{in} - (\rho C_p)_c q_c T_j^{out} + UA(T_r - T_j) + U_a A_a(T_a - T_j) \tag{16}$$

where ΔH, U, A, and Q_{loss} denote the heat of reaction for propagation, the overall heat-transfer coefficient, the heat-exchange area, and the rate of heat loss, respectively. Further, the subscripts j, c, and a represent the jacket, the heating−cooling water, and ambient air, respectively.

3. Extended Kalman Filter-Based NLMPC

We assume that the process model is represented by the following nonlinear differential equations:

$$\dot{x} = f(x, u, d) \tag{17}$$

$$y = g(x, d) \tag{18}$$

Here x, u, d, and y denote the state vector, the manipulated input vector, the unmeasured disturbance vector, and the output vector, respectively.

The basic idea of the EKF is to perform linearization at each time step to approximate the nonlinear system as a time-varying system affine in the variables to be estimated, and apply the linear filter theory to it. In the EKF, the discrete process model equations are linearized as follows:

$$\tilde{A}_{k-1} = \frac{\partial f(x,u,d)}{\partial x}\bigg|_{(x=x_{k-1|k-1},u=u_{k-1},d=C^w x^w_{k-1|k-1})} \quad (19)$$

$$A_{k-1} = \exp(\tilde{A}_{k-1} t_s) \quad (20)$$

$$\tilde{B}^d_{k-1} = \frac{\partial f(x,u,d)}{\partial d}\bigg|_{(x=x_{k-1|k-1},u=u_{k-1},d=C^w x^w_{k-1|k-1})} \quad (21)$$

$$B^d_{k-1} = \int_0^{t_s} \exp(\tilde{A}_{k-1}\tau)\,d\tau \cdot \tilde{B}^d_{k-1} \quad (22)$$

$$\tilde{B}^u_{k-1} = \frac{\partial f(x,u,d)}{\partial u}\bigg|_{(x=x_{k-1|k-1},u=u_{k-1},d=C^w x^w_{k-1|k-1})} \quad (23)$$

$$B^u_{k-1} = \int_0^{t_s} \exp(\tilde{A}_{k-1}\tau)\,d\tau \cdot \tilde{B}^u_{k-1} \quad (24)$$

$$C_k = \frac{\partial g(x,d)}{\partial x}\bigg|_{(x=x_{k|k-1},d=C^w x^w_{k|k-1})} \quad (25)$$

$$C^d_k = \frac{\partial g(x,d)}{\partial d}\bigg|_{(x=x_{k|k-1},d=C^w x^w_{k|k-1})} \quad (26)$$

Model predictive control algorithms use a model to predict the effect of past control inputs on the process output and then calculate the current and future control actions required to move the predictive process outputs along their desired set point trajectories. The prediction equation for p sampling intervals into the future can be written as eq 27. While y^c is a controlled variable and is expressed as $h(x,d)$, $F_{jts}(x_{k|k},u_{k-1},C^w(A^w)^j x^w_{k|k}|_{0\le i \le j})$ represents the terminal states obtained by integrating ordinary differential equation (ODE) eq 17 for j sampling intervals. Also, H_k and H^d_k denote the Jacobian matrixes of the output equation.

$$\begin{bmatrix} y^c_{k+1|k} \\ y^c_{k+2|k} \\ \vdots \\ y^c_{k+p|k} \end{bmatrix} = \begin{bmatrix} I \\ I \\ \vdots \\ I \end{bmatrix}(h(x_{k|k},C^w x^w_{k|k}) - H_k x_{k|k} - H^d_k C^w x^w_{k|k}) +$$
$$\begin{bmatrix} H_k F_{ts}(x_{k|k},u_{k-1},C^w x^w_{k|k}) \\ H_k F_{2ts}(x_{k|k},u_{k-1},C^w(A^w)^i x^w_{k|k}|_{0\le i \le 1}) \\ \vdots \\ H_k F_{pts}(x_{k|k},C^w(A^w)^i x^w_{k|k}|_{0\le i \le p-1}) \end{bmatrix} +$$
$$\begin{bmatrix} H^d_k C^w A^w \\ H^d_k C^w (A^w)^2 \\ \vdots \\ H^d_k C^w (A^w)^p \end{bmatrix} x^w_{k|k} +$$
$$\begin{bmatrix} H_k B^u_k & 0 & \cdots & 0 \\ H_k(A_k B^u_k + B^u_k) & H_k B^u_k & \cdots & 0 \\ \vdots & \vdots & \ddots & \vdots \\ \sum_{i=0}^{p-1} H_k A_k^i B^u_k & \cdots & \cdots & H_k B^u_k \end{bmatrix}\begin{bmatrix} \Delta u_k \\ \Delta u_{k+1} \\ \vdots \\ \Delta u_{k+m-1} \end{bmatrix} \quad (27)$$

The above prediction equation can be simplified as follows:

$$Y_{k+1|k} = \mathcal{T}(h(x_{k|k},C^w x^w_{k|k}) - H_k x_{k|k} - H^d_k C^w x^w_{k|k}) +$$
$$S^x_k(x_{k|k},u_{k-1},x^w_{k|k}) + S^{xw}_k x^w_{k|k} + S^u_k \Delta U_k = Y^0_{k+1|k} + S^u_k \Delta U_k \quad (28)$$

where the term $Y^0_{k+1|k}$ can be calculated from the state estimates by performing integration of the nonlinear ODE and calculating the Jacobian matrixes. Here, S^u_k is a matrix that must be recomputed at each time step on the basis of the updated Jacobian matrixes. The EKF-based nonlinear model predictive controller (NL-MPC) is well described in the literature.[8,12]

On the basis of the multistep prediction in eq 28, a sequence of optimal control moves can be computed, which minimizes a chosen norm of the expected future error. The objective function and constraints for the EKF-based NLMPC are as follows:

$$\min_{\Delta U_k} ||\Lambda^y[Y_{k+1|k} - R_{k+1|k}]||_2^2 + ||\Lambda^u \Delta U_k||_2^2 \quad (29)$$

$$u^{low}_{k+l} \le u_{k+l} \le u^{high}_{k+l}, \quad 0 \le l \le m-1 \quad (30)$$

$$-\Delta u^{max}_{k+l} \le \Delta u_{k+l} \le \Delta u^{max}_{k+l}, \quad 0 \le l \le m-1 \quad (31)$$

$$y^{low}_{k+l} \le y^c_{k+l} \le y^{high}_{k+l}, \quad 0 \le l \le p \quad (32)$$

where $R_{k+1|k}$ is the future reference vector for y^c available at time k. Here, Λ^y and Λ^u are weighting matrixes that are chosen as diagonal matrixes in most cases.

In the presence of constraints, the optimization can be solved via quadratic programming. A detailed solution procedure was studied by Ricker.[13] The control moves are implemented in receding horizon fashion; that is, only the first move is implemented and the optimization procedure is repeated at the next sampling time.

4. Experimental Section

4.1. Experimental System. Figure 1 shows the schematic diagram of the continuous MMA polymerization reactor system used in this study. The jacketed glass overflow reactor has a capacity of 1 L and is equipped with a stirrer for the mixing of the reactants. An inverter is adopted to maintain the stirring speed at 300 rpm. Heating and cooling of the reaction mixture are carried out with heating–cooling water in the jacket. The valve stem positions of the hot and cold water lines were adjusted, in a cascade control configuration, in such a way that the jacket inlet temperature was kept equal to the desired value specified by the master controller.

A variable-speed, remote set point pump is used for pumping the solution of monomer, solvent, and initiator into the reactor. This is a piston-operated metering pump from FMI LAB (model QVG50). The speed of the pump motor is controlled with a stroke rate controller (model V200). The reaction product flows out of the reactor via an overflow line. To measure the density and viscosity of the reaction mixture, the circulation line is attached to the reactor. The product is circulated by the
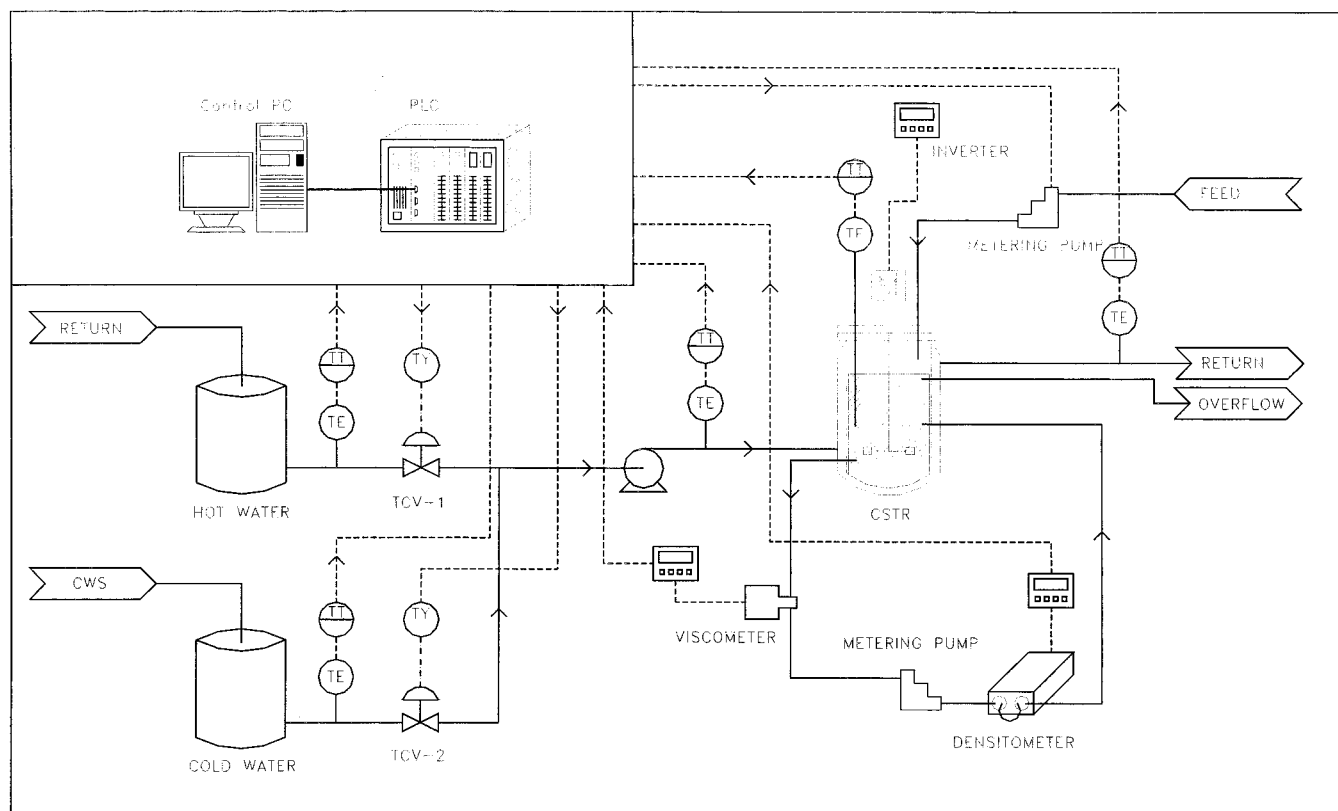
Figure 1. Schematic diagram of the experimental setup for the control of a continuous MMA polymerization reactor system.

diaphragm metering pump through the circulation line, in which the on-line densitometer and viscometer are installed.

4.2. On-Line Measurements. The essential element required for good polymerization process control is an adequate array of process sensors and good process monitoring algorithms. The feedback control of a variable is impossible unless it can be measured or estimated. With more process sensors applied in practice, one can have a better understanding of the process and conduct better process monitoring and control.

The density of the polymer can be used effectively to follow the course of polymerization and to examine the variation of monomer conversion X, which is defined as follows:

$$X = \frac{v_p \rho_p}{v_m \rho_m + v_s \rho_s + v_p \rho_p} = \frac{V_p \rho_p}{V \rho} \tag{33}$$

where v_i denotes the volume fraction of each component.

After going through several steps of algebraic manipulation, one can express the measured density ρ_d of the reaction mixture, which is measured at the on-line densitometer, in terms of the conversion and the densities of individual components; that is,

$$\rho_d = \frac{1}{\frac{1}{\rho_m} + X\left(\frac{1}{\rho_p} - \frac{1}{\rho_m}\right) + W_{sf}\left(\frac{1}{\rho_d} - \frac{1}{\rho_m}\right)} \tag{34}$$

in which the densities of each component are to be determined at the measuring temperature. Here, W_{sf} represents the weight fraction of solvent in the reactor. Since the consumption of solvent is negligible, W_{sf} may be assumed to remain constant. Equation 34 may be rearranged to express the conversion as a function of

the density measured by the on-line densitometer.

$$X = \frac{\left(\frac{1}{\rho_d} - \frac{1}{\rho_m}\right) - W_{sf}\left(\frac{1}{\rho_s} - \frac{1}{\rho_m}\right)}{\left(\frac{1}{\rho_p} - \frac{1}{\rho_m}\right)} \tag{35}$$

Since many polymer properties are related to the molecular weight distribution (MWD), it would be desired to measure the MWD on-line. Gel permeation chromatography (GPC) has been extensively used for the measurement of the MWD. However, it is rarely used for the on-line measurement because this measurement involves a time delay of about 15 min. An alternative to measure the weight-average molecular weight is to determine the molecular weight from the viscosity. It is well-known that the weight-average molecular weight is closely related to the viscosity, temperature, and conversion of the reaction mixture.

For the on-line measurement of molecular weights, the state estimation method has been used by various authors.[14−16] In addition, some correlations have been reported to show the relationship between the specific viscosity (η_{sp}) measured by the viscometer and the intrinsic viscosity ($[\eta]$). Table 1 summarizes the correlations suggested by Huggins, Martin, and Lyons, respectively.[17]

The empirical equation developed in this study is also listed in Table 1, for which b and k_H may be treated as the curve-fitting parameters and C indicates the mass concentration (g/mL) of the polymer in the reactor. It can be obtained by using the data from the on-line densitometer; that is, $C = X\rho_d$. In comparison to the Lyon's correlation, the empirical equation of this study shows that the intrinsic viscosity is much less sensitive

Table 1. Viscosity Correlations Reported in the Literature and Proposed in This Study

equation	ref
$\dfrac{\eta_{sp}}{C[\eta]} = 1 + k_H[\eta]C$	Huggins
$\eta_{sp}/C[\eta] = \exp k_H[\eta]C$	Martin
$\eta_{sp}/C[\eta] = \exp k_H[\eta]C/(1 - bC)$	Lyon
$\eta_{sp} = C^{0.8}[\eta]\exp k_H[\eta]C^{0.8}/(1 - bC^{0.8}) -$ $(C^{0.8})^2[\eta]^2\exp k_H[\eta]C^{0.8}/(1 - bC^{0.8})$	this work

Table 2. Reference Conditions for the Continuous MMA Polymerization Reactor

item	value
initial charge	
monomer	450 mL
solvent	450 mL
initiator	4.5 g
feed concentration	
monomer	4.65 mol/L
solvent	5.04 mol/L
initiator	0.02 mol/L
operating conditions	
reactor temperature	70−80 °C
feed flow rate	5−15 mL/min

to the change in the polymer concentration C and correlates the experimental data very well.

The weight-average molecular weight can be calculated if the intrinsic viscosity $[\eta]$ determined by the correlation is used in the Mark−Houwink equation

$$[\eta] = K(M_w)^a \tag{36}$$

where K and a are Mark−Houwink constants, which may be assumed to be independent of the temperature. The values of the constants K and a are given as 6.75 $\times 10^{-3}$ and 0.72, respectively.[18]

4.3. Experimental Procedure. Ethyl acetate (EA), benzoyl peroxide (BPO), and methyl methacrylate (MMA) are used as solvent, initiator, and monomer, respectively. The inhibitor contained in the monomer is eliminated by using a 0.1 M NaOH solution. Nitrogen is bubbled through the reaction mixture for about 30 min to purge the monomer and solvent of oxygen. The reactor temperature is raised to the desired starting temperature, and then the purified initiator dissolved in solvent is fed to start the polymerization. Also, the switch of the feeding pump is turned on to feed the solution of monomer, solvent, and initiator into the reactor. The set of reference conditions for the experiment is given in Table 2. The reaction mixture is sampled at successive times, and the conversion is measured by the gravimetric method, while the average molecular weights are measured by gel permeation chromatography. The conversion and the weight-average molecular weight are also determined from the on-line measurements of the density and the viscosity of the reaction mixture.

5. Control System Design

5.1. Process Model. The state vector is composed of the concentrations of initiator, monomer, and solvent, respectively, and the moments of dead polymer concentrations and reactor and jacket temperatures. The kth moment of the dead polymer concentration is much larger than that of the living polymer concentration.

Therefore, the quasi-steady-state approximation is valid for the moments of the living polymer concentration. The primary target is the regulation of the conversion and the weight-average molecular weight, which are measured on-line. Of course, the reactor temperature is directly measured. The manipulated variables are the jacket inlet temperature and the feed flow rate. It is very hard to acquire precise values of UA, U_aA_a, and Q_{loss}. Thus, the lumped terms (d_1 and d_2) may be added to the process model in eqs 15 and 16. These unmeasured disturbances can be modeled by integrated white noise in such a way that the bias of the states can be corrected. Now, the state vector x, the manipulated input vector u, the unmeasured disturbance d, and the output vector y are defined, respectively, as

$$x = \left[\frac{1}{I_f}\ \frac{M}{M_f}\ \frac{S}{S_f}\ \frac{F_0}{F_{00}}\ \frac{F_1}{F_{10}}\ \frac{F_2}{F_{20}}\ \frac{T_r}{T_a}\ \frac{T_j}{T_a}\right]^T \tag{37}$$

$$u = \left[\frac{T_j^{in}}{T_a}\ \frac{q_f}{q_{f0}}\right]^T, \quad y = \left[\frac{T_r}{T_a}\ X\ M_w\right]^T \tag{38}$$

$$d = [d_1\ d_2]^T \tag{39}$$

5.2. Design Parameters. The initial values of the estimation error covariance matrix and the covariance matrix of measurement noise are chosen as follows:

$$\Sigma_{0|0} = \\ \mathrm{diag}(10^{-10}\ 10^{-10}\ 10^{-10}\ 10^{-4}\ 10^{-4}\ 10^{-10}\ 10^{-10}\ 10^{-2})$$

$$R^y = \mathrm{diag}(10^{-6}\ 10^{-8}\ 10^{-2})$$

The covariance matrix of the plant noise is taken as the unit matrix, that is, $R^w = I$, and other design parameters are specified as $p = 30$ and $m = 5$. The main tuning parameters are the prediction horizon (p), the control horizon (m), the output weighting matrix, and the input weighting matrix. As the prediction horizon increases, the MPC can predict further into the future and the performance gets improved. However, the calculation time becomes longer, which results in a more sluggish response. We have chosen the prediction horizon and the control horizon considering both the calculation time and the performance of the controller. The weighting matrixes have been selected by trial and error methods. Also, the tuning was carried out in a tradeoff manner within the MPC by optimization.

6. Results and Discussion

6.1. Model Validation and On-Line Measurement. The polymerization reaction experiment was conducted and the polymer properties were measured both on-line and off-line in such a way that the proposed model and measurement technique could be validated. Figure 2 shows the comparison between the experimental and simulation results when the set points of the reactor temperature and the feed flow rate undergo a series of step changes, respectively. The two are in fairly good agreement not only in terms of the conversion but also in view of the molecular weights. Therefore, it may be concluded that the model developed in this study is adequate to be used for a model predictive controller.

The on-line measurement values of conversion and weight-average molecular weight are presented in Fig-
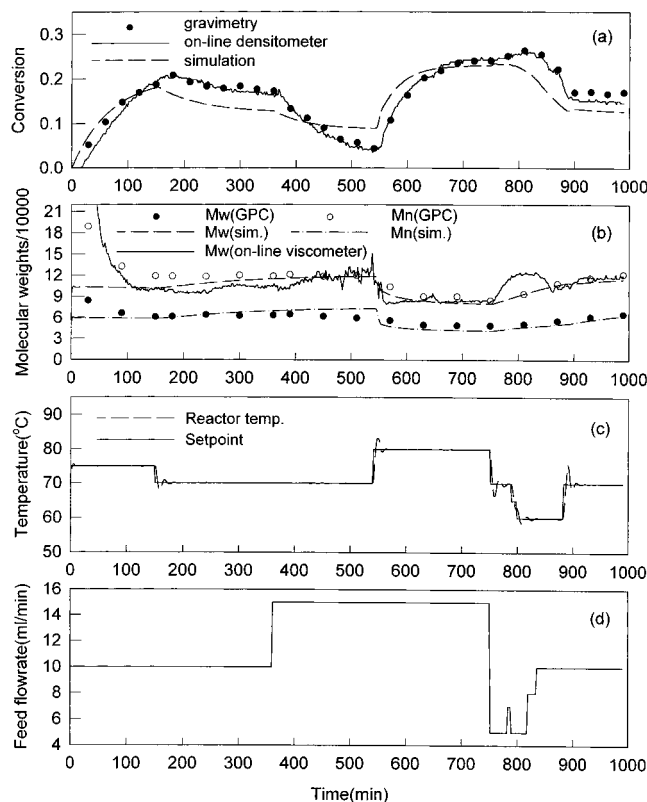
Figure 2. Histories of conversion and molecular weights when the set points of the reactor temperature and the feed flow rate undergo a series of step changes, respectively (case 1).
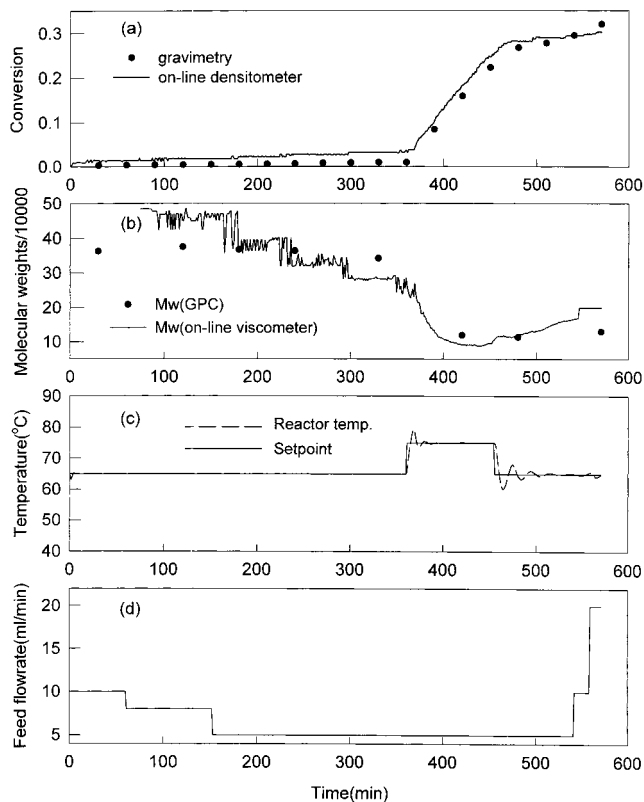

Figure 3. Histories of conversion and molecular weights when the set points of the reactor temperature and the feed flow rate undergo a series of step changes, respectively (case 2).

ure 2 (a and b). Clearly, the values are found to agree well with the off-line measurement values. Hence, it is justified to use the measured values for on-line state estimation.

Figure 3 presents the experimental result when the reactor temperature is low. It is noticed that the conversion is very low, while the weight-average molecular weight is very high. The value of the weight-average molecular weight is about 400 000 g/mol. Here again, the on-line measurements of the weight-average molecular weight are found to be in good agreement with the off-line measurement.

6.2. Controller Performance: SISO Case. In this case, the manipulated variable is the jacket inlet temperature, and the controlled variable is the conversion. The weighting factors are 1 for the output and 2.5 for the input. The upper and lower bounds of the jacket inlet temperature are 85 and 50 °C, respectively.

The performance of the proportional-integral-derivative (PID) controller for the control of conversion is shown in Figure 4, where the tuned parameters are K_c = 300, τ_I = 1.66 min, and τ_D = 0.05 min, respectively. For the set point of conversion of 0.1, the controller quickly drives the conversion to its set point. However, when the set point is raised to 0.2, the response is very slow and the conversion reaches its set point after about 200 min. Obviously, it is required to take into account the nonlinearity of the process and the variation of the tuning parameters (such as gain scheduling).

Figure 5 presents the performance of the linear MPC, which is designed by using a linear model derived at the nominal steady-state. The servo response appears to be even worse than that obtained with the PID controller. The set point change causes large, poorly damped oscillation in conversion, as shown in part a of
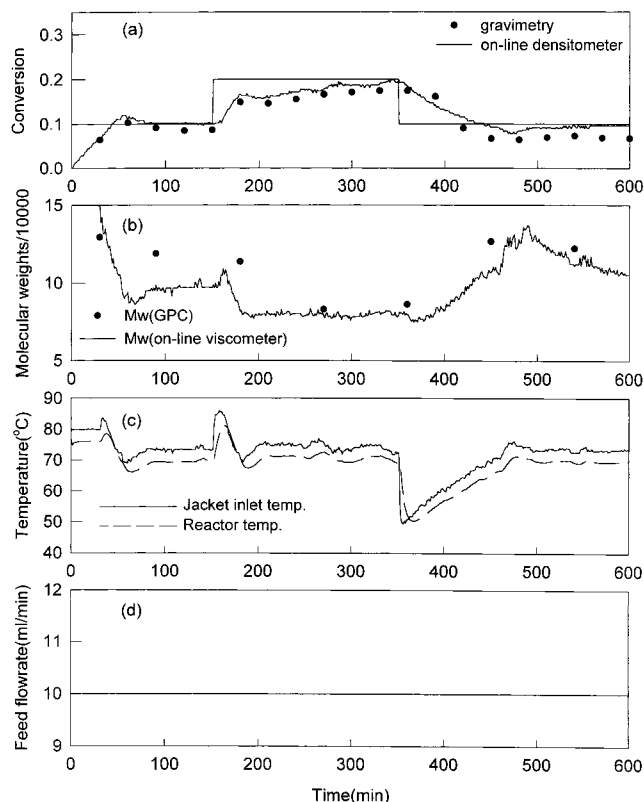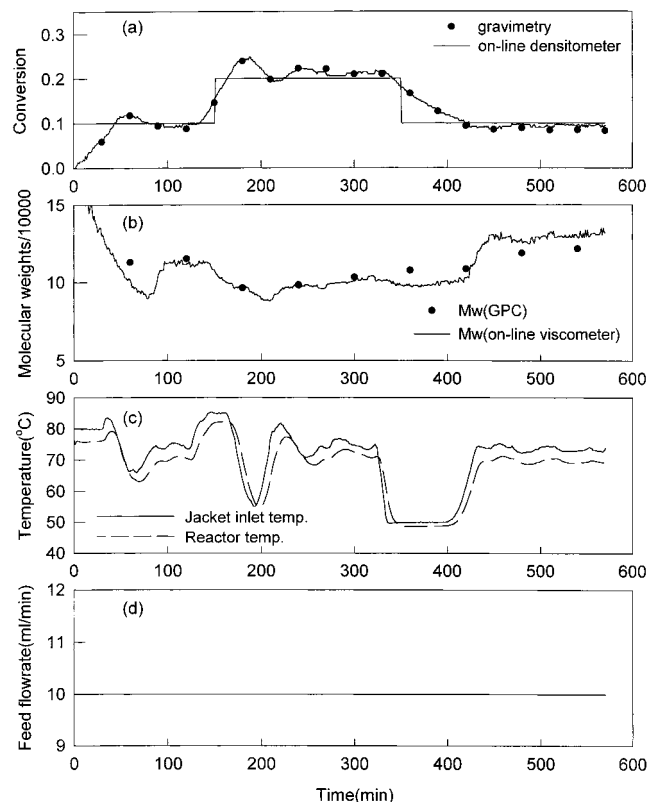

Figure 4. Servo and regulatory performances of the PID controller for step changes in the set point for conversion.

Figure 5. Furthermore, part c indicates that the reactor temperature does not reach its steady-state value.

When the EKF-based NLMPC is employed for the same set point changes as in the previous cases, the
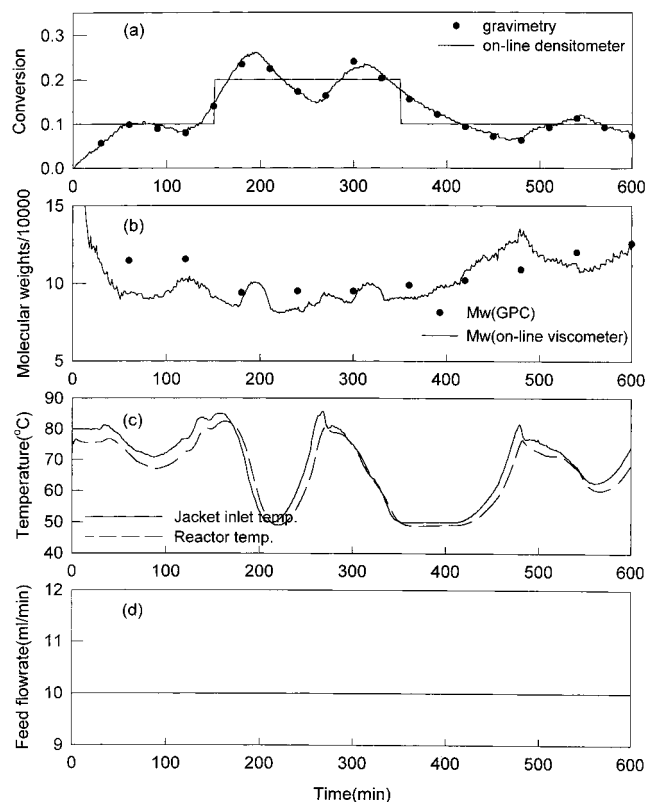
Figure 5. Servo and regulatory performances of the linear MPC for step changes in the set point for conversion.

Figure 6. Servo and regulatory performances of the EKF-based NLMPC for step changes in the set point for conversion.

servo and regulatory performances are shown in Figure 6. Within the first 100 min, the controller drives the conversion to its set point of 0.1. For the increase in the conversion set point to 0.2, the controller output (the set point of the jacket inlet temperature) increases to

Table 3. Comparison of Various Control Criteria among the PID Controller, the LMPC, and the NLMPC

	ISE	IAE	ITAE
PID	0.657	13.57	3384.7
LMPC	0.571	14.40	3911.0
NLMPC	0.388	9.99	2293.1

its upper bound at 85 °C and subsequently varies around its steady-state value as one can see in part c of Figure 6. Part b shows the variation of the weight-average molecular weight, where the curve and the filled keys represent the on-line and off-line data, respectively. It is noticed that the two are in good agreement.

For quantitative comparison, three different criteria for good control were tested; that is, integral of the square error (ISE), integral of the absolute value of the error (IAE), and integral of the time-weighted absolute error (ITAE). The results are summarized in Table 3. All three criteria clearly indicate that the NLMPC is superior to the PID controller or the LMPC. It is evident that the quality of the polymer product can be controlled by using the NLMPC.

We have used the same tuning parameters for the NLMPC and LMPC to compare the performance between the two. The performance of the LMPC may be improved by fine-tuning. However, it may be more difficult to tune the LMPC than the NLMPC, since the LMPC is based on the local linear model.

6.3. Controller Performance: MIMO Case. In this case, the manipulated variables are the jacket inlet temperature and the feed flow rate whereas the controlled variables are the conversion and the weight-average molecular weight.

The upper and lower bounds of the feed flow rate are 30 and 5 mL/min, respectively. The weighting matrixes are diag(10, 0.05) for the output and diag(30, 2) for the input. The other parameters are the same as those for the case of SISO.

In Figure 7, parts a and b present the profiles of the controlled outputs when there are step changes in the set points of the conversion and the molecular weight. The corresponding profiles of the jacket inlet temperature and the feed flow rate are shown in parts c and d. The set point of the molecular weight is changed from 120 000 g/mol to 150 000 g/mol at 350 min, while the set point of the conversion remains unchanged.

Since the reactor has interactive dynamics, the controller increases the feed flow rate (to increase the weight-average molecular weight) and also increases the jacket inlet temperature (to maintain the conversion at 0.1) simultaneously to compensate for the interaction. However, the controller cannot fully compensate for the effect of the set point change in the molecular weight, and thus the conversion slightly oscillates before returning to its set point at about 500 min.

When the conversion set point increases to 0.2 and the set point for the molecular weight goes down to 90 000 g/mol at 600 min, the transition turns out to be really fast and smooth and the controller performance is found to be remarkably good.

7. Conclusions

An EKF-based nonlinear model predictive controller was implemented experimentally to control the conversion and the weight-average molecular weight in a continuous MMA polymerization reactor. For this, a
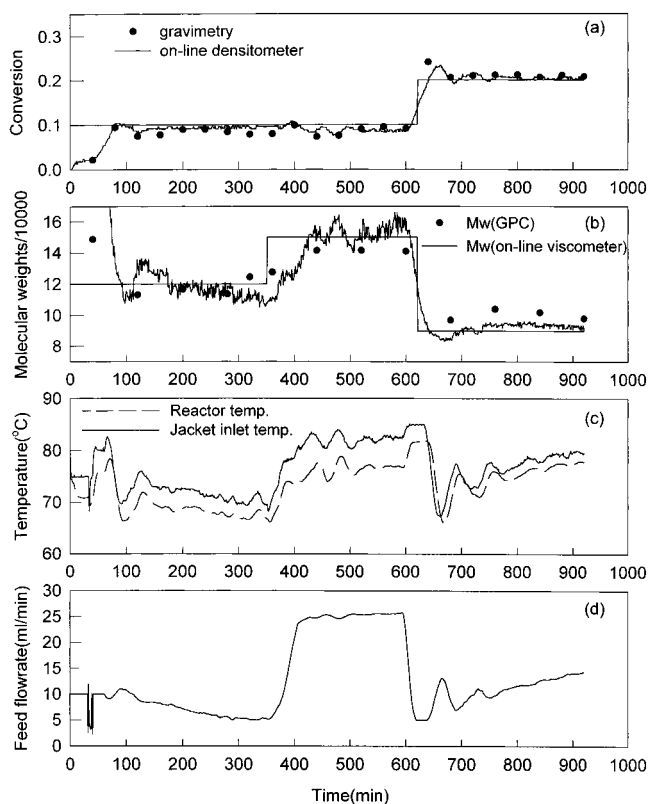
Figure 7. Servo and regulatory performances of the EKF-based NLMPC for step changes in the set points for both conversion and weight-average molecular weight.

mathematical model was developed for a continuous reactor in which free radical polymerization of methyl methacrylate (MMA) occurred. To measure the properties of the polymer on line, the densitometer and the viscometer were utilized.

On the basis of the experimental results, it is concluded that the EKF-based NLMPC performs better than the PID controller or the LMPC in the sense of better regulation and less oscillation. Despite the complex and nonlinear features of the polymerization reaction system, the EKF-based NLMPC performed quite satisfactorily for the property control of the continuous polymerization reactor. It seems evident that the proposed control strategy may be applied to other continuous polymerization processes to minimize the production of off-spec polymer.

Acknowledgment

Literature Cited

(1) Congalidis, J. P.; Richards, J. R.; Ray, W. H. Feedforward and Feedback Control of a Solution Copolymerization Reactor. *AIChE J.* **1989**, *35*, 891.

(2) Adebekun, D. K.; Schork, F. J. Continuous Solution Polymerization Reactor Control. 1. Nonlinear Reference Control of Methyl Methacrylate Polymerization. *Ind. Eng. Chem. Res.* **1989**, *28*, 1308.

(3) Adebekun, D. K.; Schork, F. J. Continuous Solution Polymerization Reactor Control. 2. Estimation and Nonlinear Reference Control during Methyl Methacrylate Polymerization. *Ind. Eng. Chem. Res.* **1989**, *28*, 1846.

(4) Elicabe, G. E.; Meira, G. R. Model Reference Adaptive Control of a Continuous Polymerization Reactor Under Periodic Operation. *Polym. Eng. Sci.* **1989**, *29*, 374.

(5) Kurtz, M. J.; Henson, M. A. Constrained Output Feedback Control of a Multivariable Polymerization Reactor. Proceedings of the American Control Conf., New Mexico, June 1997; p 2950.

(6) Soroush, M.; Kravaris, C. Multivariable Nonlinear Control of a Continuous Polymerization Reactor: an Experimental Study. *AIChE J.* **1993**, *39*, 1920.

(7) Mutha, R. K.; Cluett, W. R.; Penlidis, A. On-line Nonlinear Model-Based Estimation and Control of a Polymer Reactor. *AIChE J.* **1997**, *43*, 3042.

(8) Lee, J. H.; Ricker, N. L. Extended Kalman Filter Based Nonlinear Model Predictive Control. *Ind. Eng. Chem. Res.* **1994**, *33*, 1530.

(9) Reichert, K. H.; Geiseler, W. *Polymer Reaction Engineering*; Hanser Publishers: New York, 1983.

(10) Schmidt, A. D.; Ray, W. H. The Dynamic Behavior of Continuous Polymerization Reactors-I. Isothermal Solution Polymerization in a CSTR. *Chem. Eng. Sci.* **1981**, *36*, 1401.

(11) Ahn, S.-M.; Chang, S.-C.; Rhee, H.-K. Application of Optimal Temperature Trajectory to Batch PMMA Polymerization Reactor. *J. Appl. Polym. Sci.* **1998**, *69*, 59.

(12) Ahn, S.-M.; Park, M.-J.; Rhee, H.-K. Property Control in a Continuous MMA Polymerization Reactor using EKF based Nonlinear Model Predictive Controller. Proceedings of the 13th Korea Automatic Control Conf., Pusan, October 1998; p 458.

(13) Richer, N. L. The Use of Quadratic Programming for Constrained Internal Model Control. *Ind. Eng. Chem. Process Des. Dev.* **1985**, *24*, 925.

(14) Mankar, R. B.; Saraf, D. N.; Gupta, S. K. On-Line Optimizing Control of Bulk Polymerizations: 1. Development of a Software Sensor. *Ind. Eng. Chem. Res.* **1998**, *37*, 2436.

(15) Ram, G. B. B.; Gupta, S. K.; Saraf, D. N. Free-Radical Polymerizations Associated with the Trommsdorff Effect Under Semibatch Reactor Conditions. IV. On-Line Inferential-State Estimation. *J. Appl. Polym. Sci.* **1997**, *64*, 1861.

(16) Ellis, M. F.; Taylor, T. W.; Jensen, K. F. On-Line Molecular Weight Distribution Estimation and Control in Batch Polymerization. *AIChE J.* **1994**, *40*, 445.

(17) Lyons, P. F.; Tobolsky, A. V. Viscosity of Polypropylene Oxide Solutions over the Entire Concentration Range. *Polym. Eng. Sci.* **1970**, *10* (1), 1.

(18) Brandrup, J.; Immergut, E. H. *Polymer Handbook*; Wiley: New York, 1989.